Mechanistic Insights into Sky1p, a Yeast Homologue of the Mammalian SR Protein Kinases†

Brandon E. Aubol,‡ Brad Nolen,‡ Don Vu,‡ Gourisankar Ghosh,‡ and Joseph A. Adams*,§

Department of Chemistry and Biochemistry and Department of Pharmacology, University of California, San Diego, La Jolla, California, 92093

Received March 26, 2002; Revised Manuscript Received June 6, 2002

ABSTRACT: The SRPK family is distinguished from typical eukaryotic protein kinases by several unique structural features recently elucidated by X-ray diffraction methods [Nolen et al. (2001) *Nat. Struct. Biol. 8*, 176−183]. To determine whether these features impart unique catalytic function, the phosphorylation of the physiological Sky1p substrate, Npl3p, was monitored using steady-state and pre-steady-state kinetic techniques. While Sky1p has a low apparent affinity for ATP compared to other protein kinases, it binds Npl3p with very high affinity. The latter is achieved through a combination of local and distal factors in the protein substrate. The phosphoryl donor ATP has access to the nucleotide pocket in the absence or presence of Npl3p, indicating that a large protein substrate does not enforce an ordered addition of ligands. Sky1p binds two Mg^{2+}—the first is essential whereas the second further enhances catalysis. While the turnover number is low (0.5 s^{-1}), Npl3p is rapidly phosphorylated in the active site (40 s^{-1}) based on single turnover experiments. These results indicate that Sky1p employs a catalytic pathway involving fast phosphoryl transfer followed by slow net release of products. These studies represent the first kinetic investigation of a member of the SRPK family and the first pre-steady-state kinetic study of a protein kinase using a natural protein substrate.

An essential step in the maturation of eukaryotic pre-mRNA is the removal of intervening sequences (introns) from the coding sequences (exons). This pre-mRNA splicing takes place in a dynamic assembly of five small nuclear RNAs (snRNAs)[1] and other proteins known as the spliceosome (*1*−*4*). As well as snRNPs, many non-snRNPs such as SR proteins play critical roles in splicing. SR proteins have been shown to function in vitro as essential factors required for spliceosome assembly and alternative splice site selection. SR proteins are characterized by one or more RNA recognition motifs (RRMs), as well as an RS domain rich in serine and arginine dipeptide repeats. SR proteins use their RNA recognition motifs to bind and commit pre-mRNA molecules to the splicing pathway, whereas the RS domains mediate specific protein−protein interactions during the spliceosome assembly step.

The maturation of mRNA is regulated by a class of enzymes known as SR protein kinases (SRPKs) (*5*−*8*). In vitro, a cycle of phosphorylation and dephosphorylation is imperative for splicing to occur. The phosphorylation of SR proteins is required for spliceosome assembly, and a dephosphorylation step is necessary for the splicing event to occur (*9*−*11*). SRPKs are highly homologous across species (∼50% identity between human and yeast), and are characterized by a large spacer insert of about 250−300 residues (referred to as spacer region) within the kinase core. It has been shown that this spacer is important for subcellular localization as well as cell viability in yeast (*12*). In *Saccharomyces cerevisiae*, Sky1p has been identified as the only kinase highly homologous to human SRPKs. Although multiple proteins in *Saccharomyces cerevisiae* have the ability to become phosphorylated by Sky1p, the SR protein Npl3p is the only one that is well characterized. Npl3p is a shuttling protein involved with mRNA transport, and is phosphorylated at a single serine within the C-terminus (*12*). Npl3p contains two RRM domains and a C-terminal RGG/RS domain. The latter domain contains eight RS dipeptide repeats although only the last one is phosphorylated by Sky1p (*13*). Recent biochemical data indicate that Sky1p-mediated phosphorylation of Npl3p is imperative for the viable transport of this SR protein to the nucleus where it binds to mRNA and transports it back to the cytoplasm (*12, 13*).

SRPKs represent a unique enzyme group within the larger protein kinase family. All members of the SRPK family, including Sky1p, are constitutively active and display remarkable substrate specificity (*5, 7, 8, 14*). Recently, the X-ray crystal structure of Sky1p lacking the spacer insert and a large portion of the N-terminus (Sky1pΔNS, Figure 1) was solved, providing unique insights into the SRPKs (*15*). In addition to the unique spacer insert located between β

† This work was supported by grants from the NSF (111068) and NIH (CA 75112) to J.A.A., by an Alfred Sloan Foundation and Cancer Research Program grant to G.G., and by a training grant to B.E.A. (GM 07752).

* To whom correspondence should be addressed. Telephone: (858) 822-3360. Fax: (858) 822-3361. E-mail: joeadams@chem.ucsd.edu.

‡ Department of Chemistry and Biochemistry.

§ Department of Pharmacology.

[1] Abbreviations: AMPPNP, 5′-adenylylimidodiphosphate; Csk, C-terminal Src kinase; Her-2, human epidermal growth factor receptor; PKA, cAMP-dependent protein kinase; RGG, arginine- and glycine-rich; RRM, RNA recognition motif; RS domain, domain rich in arginine and serine residues; Sky1p, SR kinase in yeast; Sky1pΔNS, Sky1p lacking the spacer insert and N-terminus; snRNAs, small nuclear RNAs; snRNPs, small nuclear ribonuclear proteins; SRPK, SR protein kinase; SR protein, splicing factor containing arginine-serine dipeptide repeats.

10.1021/bi020233y CCC: $22.00
Published on Web 07/09/2002

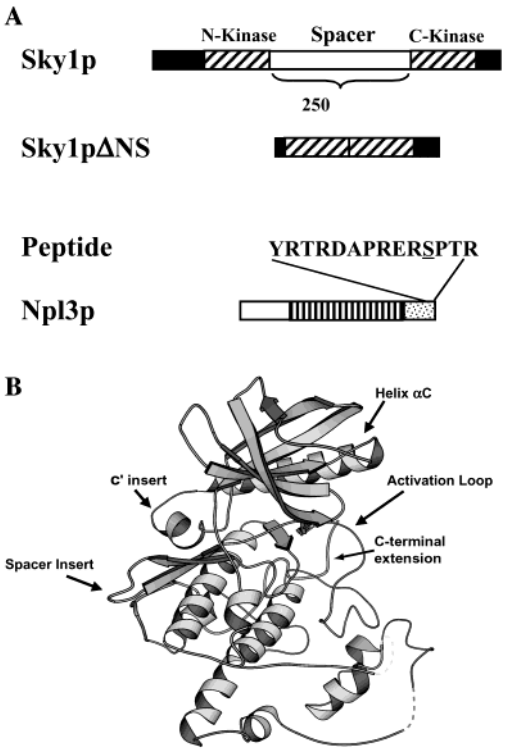

FIGURE 1: Structures of Sky1p and Npl3. (A) Domain organization. The full-length enzyme possesses a large spacer insert (250 amino acids) that bifurcates the kinase domain. The two separate portions of the complete kinase domain are labeled N-kinase and C-kinase, reflecting the N- and C-terminal sequences, The truncated enzyme, Sky1pΔNS, lacks this spacer region and a large portion of the N-terminus. The peptide represents the phosphorylation site (Ser-411) and local residues in the C-terminus of Npl3p. The phosphorylated residue in the peptide is underlined. The striped region in Npl3 contains the two RRM domains whereas the dotted region represents the RGG/RS domain. (B) X-ray structure of Sky1pΔNS. The spacer insert, not present in this structure, lies between β strands 7 and 8.

strands 7 and 8, Sky1p differs from other protein kinases in two respects. First, Sky1p contains a short helical addition directly after helix αC. Since it has been demonstrated by crystallographic and solution methods that motions in this helix are directly linked to catalytic activation (*16*−*18*), the presence of this helical addition suggests a unique role for helix αC in the SRPKs. Second, while Sky1p is not up-regulated by activation loop phosphorylation, the C-terminus directly interacts with this critical loop segment. This interaction could lock the activation loop into a productive form in the absence of other stabilizing interactions.

To investigate the catalytic properties of Sky1p, we measured the steady-state and pre-steady-state kinetic parameters of Sky1pΔNS using two substrates: the physiological yeast protein Npl3p, and a short peptide based on the single phosphorylation site in Npl3p (Figure 1). The results indicate that Sky1pΔNS requires both local and distal sequence elements for substrate recognition. The enzyme binds Npl3p and ATP randomly although the affinity of the latter is poor relative to other protein kinases. Based on single turnover experiments, the binding and phosphorylation of Npl3p are fast while the net release of products is rate-limiting. This study represents the first detailed kinetic investigation into the substrate selectivity and catalytic properties of an SRPK and, thus, will provide a critical base for evaluating the function of related enzymes involved in mRNA processing. Also, while pre-steady-state kinetic data have been previously published for three protein kinases, to date, those studies were performed using short peptide substrates rather than real physiological substrates (*19*−*21*). The data presented herein reflect the first pre-steady-state kinetic report on the phosphorylation of a natural substrate for a protein kinase.

MATERIALS AND METHODS

Materials. Adenosine triphosphate (ATP), adenosine diphosphate (ADP), 3-(*N*-morpholino)propanesulfonic acid (Mops), magnesium chloride, potassium chloride, acetic acid, DE 52 resin, and liquid scintillant were obtained from Fisher Scientific. Poly-prep chromatography columns were obtained from Bio-Rad, synthetic peptide was obtained from the Peptide and Oligonucleotide facility at the University of Southern California, 5′-adenylylimidodiphosphate (AMP-PNP) was obtained from Sigma Chemicals, and [γ-^{32}P]ATP was obtained from NEN Products.

Expression and Purification of Sky1p and Npl3p. Expression and purification of Sky1ΔNS were described previously (*15*). The yeast vector pPS811 (obtained from C. Yun and X.-D. Fu, University of California, San Diego) was used as a template to clone *NPL3P* into pET15b (Novagen) at the *Nde*I and *Bam*HI restriction sites. pET15b-*NPL3P* was transformed into BL21(DE3)RP *E. coli* (Stratagene), and cultures were grown at 37 °C in 2 L of LB broth supplemented with 200 μg/mL ampicillin and 34 μg/mL chloramphenicol for 4 h. Then 0.5 mM IPTG was added to induce protein expression. Cells were grown at 37 °C for 5 h, pelleted, and stored at −80 °C. Cells were lysed in 150 mL of lysis buffer [20 mM Tris-HCl, pH 7.5, 5 mM imidazole, 500 mM NaCl, 10% glycerol, and 0.5 mL of protease inhibitor cocktail (Sigma)]. Supernatant was loaded onto a His-bind column (Novagen) and washed with lysis buffer containing 60 mM imidazole. Protein was eluted with 30 mL of lysis buffer containing 250 mM imidazole and dialyzed twice against 2 L of 20 mM Tris-HCl, pH 7.5, 50 mM NaCl, 1 mM EDTA, 1 mM DTT, and 10% glycerol. Dialyzed protein was then loaded on a HiTrap Q Sepharose column (Amersham Pharmacia) and washed with 20 mM Tris-HCl, pH 7.5, 1 mM EDTA, 10% glycerol, 1 mM DTT, and 50 mM NaCl. Protein was eluted with the same buffer in a 10 column-volume gradient from 50 to 400 mM NaCl. Peak fractions were pooled and dialyzed twice against 2 L of 20 mM Tris-HCl, pH 7.5, 100 mM NaCl, and 1 mM DTT. Dialyzed sample was then concentrated in a Centriprep 30 (Millipore) to 9.0 mg/mL and flash-frozen. Concentration measurements for the purified proteins were made using the Gill and von Hippel method (*22*).

Column Separation Assay. The steady-state kinetic parameters in the presence of protein substrate Npl3p or substrate peptide were performed at 23 °C for 2 min in the presence of 50 mM Mops (pH 7), 4 mM free Mg^{2+}, and [γ-^{32}P]ATP (600−1000 cpm pmol^{-1}) unless otherwise stated. For time course experiments, substrate concentrations were kept constant, and only the quench times were varied. Assays were typically executed by preequilibrating the enzyme, $MgCl_2$, and ATP for 2 min, and then initiating the reaction with the addition of substrate. Total reaction volumes were 20 μL, and were quenched with 180 μL of 30% acetic acid. A portion of each reaction (180 μL) was applied to 3 mL

DE 52 columns, and washed with 5 mL of 30% acetic acid. The collected flow-through containing phosphorylated substrate was then counted on the ^{32}P channel in liquid scintillant. Control experiments were performed to determine the background phosphorylation (i.e., phosphorylation of Npl3p or substrate peptide in the presence of quench). The specific activity of [γ-^{32}P]ATP was determined by measuring the total counts of the reaction mixture. The time-dependent concentration of phosphorylated Npl3p and substrate peptide was then determined by considering the total counts per minute (CPM) of the flow-through, the specific activity of the reaction mixture, and the background phosphorylation of the flow-through as previously described.

Rapid Quench Flow Studies. The phosphorylation of Npl3p was monitored using a KinTek Corp. Quench Flow Apparatus model RGF-3 and a previously published procedure (*19*). Quench flow experiments were typically executed by loading equal volumes of enzyme, buffer (50 mM Mops, pH 7), Np13p, and magnesium chloride into one sample loop and [γ-^{32}P]ATP (600−1000 cpm pmol^{-1}) and magnesium chloride into the other in 50 mM Mops (pH 7). Unless otherwise designated in the text, the concentrations of the reactants represent those in the mixing chamber. The reactions were quenched using 30% acetic acid, and phospho-Npl3p was separated from unreacted ATP using the column separation assay. Control experiments were performed to determine the background phosphorylation (i.e., phosphorylation of Npl3p in the presence of quench) using previously published protocols (*19*). The time-dependent concentration of phospho-Npl3p was then determined by considering the total counts per minute (CPM), the specific activity of ATP, and the background phosphorylation.

Data Analysis. The steady-state kinetic parameters were obtained by plotting the initial reaction velocity versus the total substrate concentration at fixed ATP concentration or the total ATP concentration at fixed peptide concentration using eq 1:

$$v = \frac{V_{max}[S]}{K_m\left(1 + \frac{K_{ATP}}{[ATP]}\right) + [S]\left(1 + \frac{\alpha K_{ATP}}{[ATP]}\right)} \quad (1)$$

where v is the initial velocity, V_{max} is the maximum velocity, and K_{ATP} and αK_{ATP} are the K_m's for ATP at low and infinite substrate concentrations, respectively. The maximum reaction velocity was converted to k_{cat} by dividing by the total enzyme concentration. K_m reflects the apparent affinity of substrate peptide or Npl3p. The K_I for AMPPNP was measured using fixed ATP and Npl3p concentrations using eq 2:

$$v = \frac{V_{max}^{app}[ATP]}{K_{ATP}\left(1 + \frac{[AMPPNP]}{K_I}\right) + [ATP]} \quad (2)$$

where V_{max}^{app} is V_{max} at a fixed substrate or ATP concentration, K_{ATP} represents the apparent affinity of ATP, and K_I is the inhibitory constant for AMPPNP. The production of phospho-Npl3p in the rapid quench flow experiments was fitted to eq 3:

$$[P] = \alpha \times [1 - \exp(-k_b t)] + L \times t \quad (3)$$

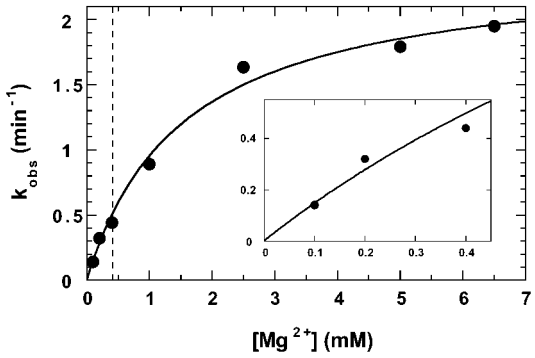

FIGURE 2: Phosphorylation of the substrate peptide as a function of the Mg^{2+} concentration. Sky1pΔNS was preequilibrated with varying concentrations of $MgCl_2$ (0.1−6.5 mM) at a fixed concentration of ATP (0.4 mM), and the reaction was initiated with 1 mM peptide. The initial reaction rate constants ($k_{obs} = v$/[E]), measured at each Mg^{2+} concentration, were fit to a hyperbolic function. The maximum rate constant is 2.4 min^{-1}. The inset shows the curve fit at Mg^{2+} levels beneath the ATP concentration.

where [P] is the concentration of phospho-Npl3p, α is the amplitude of the exponential phase, k_b is the rate constant for the exponential, L is the linear rate constant, and t is time. Equation 3 was used to fit the time dependence of phospho-Npl3p when [Npl3p] > [E]. Under conditions when [Npl3p] < [E] (single turnover conditions), L is set to zero.

RESULTS

Magnesium Dependence of Catalytic Activity. It has been shown previously that the activities of protein kinases are dependent on the total concentration of Mg^{2+} [see reference (*23*)]. To determine how Mg^{2+} affects the catalytic activity of Sky1p, the initial reaction rate constant, k_{obs}, was measured as a function of total Mg^{2+}. Figure 2 displays the reaction rate for Sky1pΔNS as a function of total Mg^{2+} at fixed concentrations of ATP (400 μM) and substrate peptide (1 mM). The reaction rate constant increases hyperbolically with total Mg^{2+}. Owing to the high affinity of Mg^{2+} for ATP in solution (K_d = 10 μM), the initial increase in catalytic rate up to the fixed concentration of ATP (dashed line in Figure 2) represents the binding of a single metal ion in the active site of the enzyme. Above this level, additional activation reflects the binding of a second Mg^{2+}. The amount of Mg^{2+} above the total concentration of ATP is called the free Mg^{2+} concentration. For Sky1p, since maximum catalytic activity is achieved at approximately 4 mM free Mg^{2+}, all kinetic studies were performed at this amount of divalent activator.

Effects of Salt on Activity. To examine the impact of ionic strength on the phosphorylation of the substrate peptide and Npl3p, the effects of increasing salt concentration were determined. Initial velocities were measured as a function of total KCl at 1 mM ATP, 4 mM free Mg^{2+}, and fixed concentrations of substrate (74 μM Npl3p or 1 mM peptide). As shown in Figure 3, there is a profound rate loss with increasing KCl concentration. Approximately 60% of the catalytic activity is lost at 100 mM KCl. A similar effect of ionic strength has been observed for Csk, a nonreceptor protein tyrosine kinase important for regulating Src family enzymes (*24*).

Available Phosphorylation Sites in Npl3p. It has been shown previously that a physiological substrate for Sky1p, Npl3p, is phosphorylated on a single serine (Ser-411) (*13*).

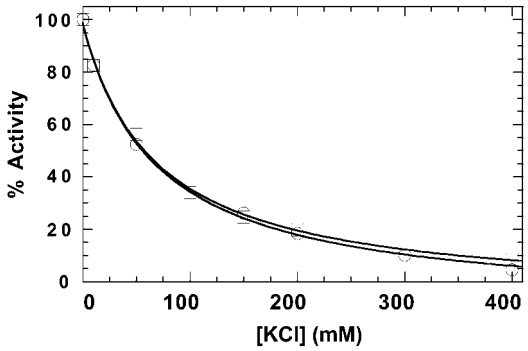

FIGURE 3: Effects of [KCl] on the percent activity of Sky1pΔNS. Initial velocities were measured in the presence of varying concentrations of KCl (0−400 mM) at 4 mM free Mg^{2+} and 1 mM ATP using 1 mM peptide (○) or 74 μM Npl3p (□).

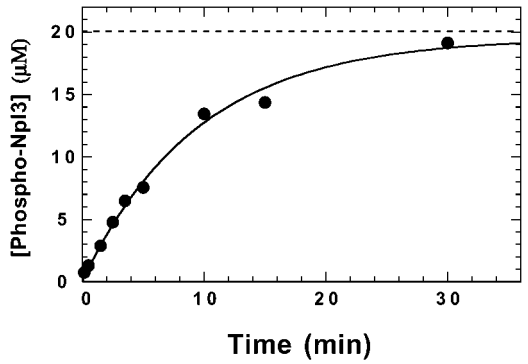

FIGURE 4: Progress curve for the phosphorylation of Npl3p. Sky1pΔNS (70 nM) was preincubated with ATP (400 μM) and 4 mM free Mg^{2+}, and the reactions were initiated with the addition of Npl3p (20 μM). The concentration of Npl3 on the *y*-axis was determined from a Bradford assay. The progress curve was fitted to an exponential function with an endpoint of 20 ± 1 μM and a rate constant of 0.10 ± 0.10 min^{-1}.

To determine the available number of phosphorylation sites in our recombinantly expressed Npl3p, we monitored the time-dependent phosphorylation of Npl3p. Figure 4 shows the incorporation of ^{32}P from [γ-^{32}P]ATP into a fixed amount of Npl3p (20 μM). The incorporation of phosphate into the substrate protein obeys a typical exponential progress curve with an endpoint of 20 μM (dashed line). Thus, a stoichiometry of 1 phosphate per Npl3 molecule is obtained, consistent with the previous reports of a single phosphorylation (*13*).

Steady-State Kinetic Parameters. The steady-state kinetic parameters for Sky1pΔNS were determined from double reciprocal plots of initial velocity versus ATP concentration at varied, fixed concentrations of substrate. Figure 5 shows plots of $1/k_{obs}$ ([E]/v) versus 1/[ATP] at varied, fixed concentrations of either substrate peptide or Npl3p. When Npl3p is used as a substrate, the lines intersect at the *x*-axis (Figure 5B), consistent with a lack of binding synergism between the nucleotide and the protein substrate. In comparison, the lines intersect below the *x*-axis using the substrate peptide (Figure 5A), a phenomenon consistent with negative binding synergism between ATP and peptide. The data were analyzed using eq 1, and the resulting steady-state kinetic parameters are listed in Table 1. Although the apparent affinity of Npl3p is about 100-fold higher than that for the substrate peptide, both substrates are turned over at similar rate constants (k_{cat}). To explain the lower activity of Sky1p at increased salt concentration (Figure 3), the steady-state kinetic parameters for Npl3p phosphorylation were measured at 100 mM KCl. Using saturating Npl3p (74 μM), k_{cat} and K_{ATP} are 0.14 ± 0.04 s^{-1} and 240 ± 50 μM for Sky1pΔNS. Thus, the effects of added salt result largely from decreases in k_{cat} with little effect on K_{ATP}.

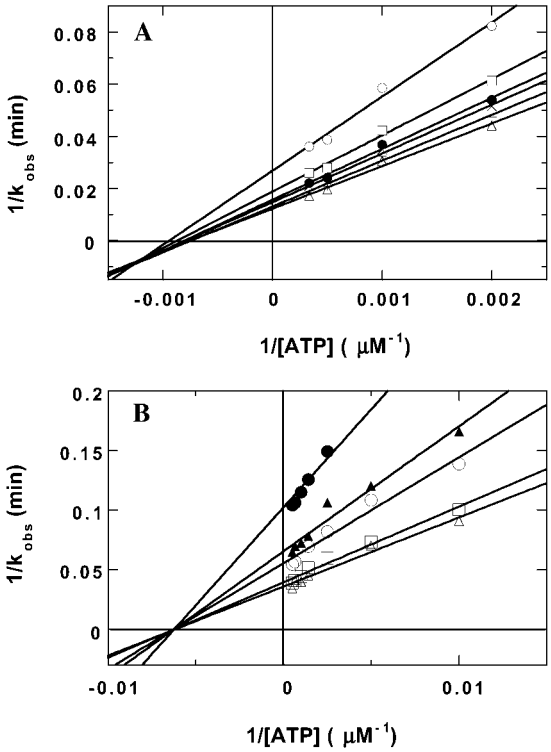

FIGURE 5: Double reciprocal plots of k_{obs} vs ATP concentration using substrate peptide and Npl3p. (A) Substrate peptide. The initial rate constants are measured as a function of varied ATP concentrations (10−2000 μM) at varied, fixed concentrations of substrate peptide [200 (○), 400 (□), 700 (●), 1000 (×), 1500 (+), and 2000 μM (△)]. (B) Npl3p. The initial rate constants are measured as a function of varied ATP concentrations (10−2000 μM) at varied, fixed concentrations of Npl3p [1 (●), 5 (▲), 7.5 (○), 20 (□), and 40 μM (△)].

Table 1: Steady-State Kinetic Parameters for Sky1pΔNS Using Npl3p and the Substrate Peptide[a]

substrate	parameter	value
peptide	k_{cat} (s^{-1})	1.0 ± 0.1
	$K_{peptide}$ (μM)	300 ± 50
	$\alpha K_{peptide}$ (μM)	1000 ± 500
	K_{ATP} (μM)	520 ± 200
	αK_{ATP} (μM)	1200 ± 500
Npl3p	k_{cat} (s^{-1})	0.5 ± 0.03
	K_{Npl3p} (μM)	3.5 ± 0.7
	K_{ATP} (μM)	200 ± 40

[a] The steady-state kinetic parameters were measured in 50 mM Mops (pH 7) buffer using 4 mM free Mg^{2+} at 23 °C. The parameters are derived from fitting eq 1 to the data in Figure 5.

Temperature Effects on Catalysis. The apparent binding affinity of ATP for Sky1p using either the natural or the peptide substrate is poor compared to other well-studied protein kinases. For example, the ATP K_m's for PKA and PKC, two classic serine-specific protein kinases, are about 10-fold lower than that for Sky1p (*25*, *26*). To better understand the ATP−Sky1p interaction, the affinities of ATP were monitored at a series of temperatures. Figure 6 shows a plot of initial velocity versus ATP concentration for Sky1pΔNS at several different temperatures. The data were

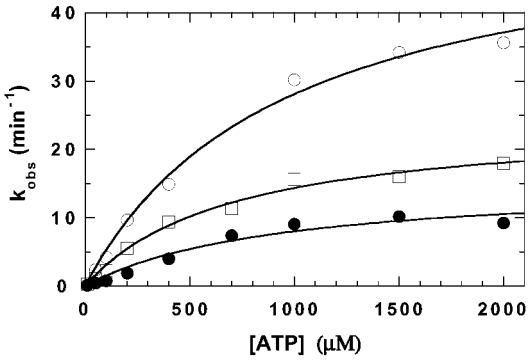

FIGURE 6: Temperature-dependent production of phosphopeptide in the presence of varying concentrations of ATP (0.01−2 mM) at 4 mM free Mg^{2+}. Sky1pΔNS (1 μM) was preequilibrated with Mg^{2+} and varying ATP concentrations, and the reaction was initiated with 1 mM substrate peptide at varied temperatures: 23 (●), 32 (□), and 37 °C (○).

recorded at 4 mM free Mg^{2+} and 1 mM peptide. The apparent K_{ATP} values at 22, 32, and 37 °C are 900, 700, and 950 μM, respectively. Thus, while there is a distinct increase in k_{obs} as a function of temperature, the apparent K_{ATP} remains unaffected.

Utilization of Nonphysiological Metal Ions. While Mg^{2+} serves as the physiological metal, many protein kinases utilize alternative divalent ions for catalysis. For example, PKA utilizes Mn^{2+} as an alternative metal although k_{cat} is reduced by about 30-fold with no change in apparent ATP binding affinity (*27*). In comparison, Csk (Src tyrosine kinase) exhibits a heightened affinity for ATP in the presence of Mn^{2+} (*28*). To gain a better understanding of the ATP−Sky1p interaction, K_{ATP} was determined at 4 mM free Mn^{2+} and 2 mM peptide concentration. The K_{ATP} for Sky1pΔNS in the presence of 4 mM free Mn^{2+} is 1300 μM (data not shown), a value that is very similar to the K_{ATP} using Mg^{2+} (Table 1). In comparison, the addition of Mn^{2+} reduced k_{cat} by 9-fold compared to Mg^{2+} (data not shown).

Inhibition Using AMPPNP. To determine whether Sky1pΔNS employs a random or ordered kinetic mechanism, inhibition studies were performed using the nonhydrolyzable ATP mimic AMPPNP. Figure 7A shows a plot of $1/k_{obs}$ ([E]/v) versus 1/[ATP] for Sky1pΔNS using varied, fixed concentrations of AMPPNP. These results are consistent with simple competitive inhibition between ATP and AMPPNP. Equation 2 was used to determine a K_I for AMPPNP of 180 ± 50 μM using Npl3p as a substrate, an affinity which is close in value to the K_m for ATP (Table 1). While AMPPNP is competitive with respect to ATP, as expected, it is noncompetitive with respect to Npl3p. As shown in Figure 7B, a plot of $1/k_{obs}$ ([E]/v) versus 1/[Npl3p] at varied, fixed concentrations of AMPPNP intersects on the *x*-axis. These results imply that AMPPNP can bind to the enzyme in the absence or presence of Npl3p. This can only occur if Sky1pΔNS utilizes a random kinetic mechanism.

Rapid Quench Flow Experiments. To define the rate-determining step for Sky1pΔNS, the phosphorylation of Npl3p was measured using rapid quench flow instrumentation. Figure 8 shows the phosphorylation of Npl3p under conditions of excess Sky1pΔNS and limiting Npl3p (single turnover conditions). The data are best represented by single exponential transients and are accordingly fit to eq 3 where $L = 0$. At all three concentrations of Npl3p (2, 5, and 8

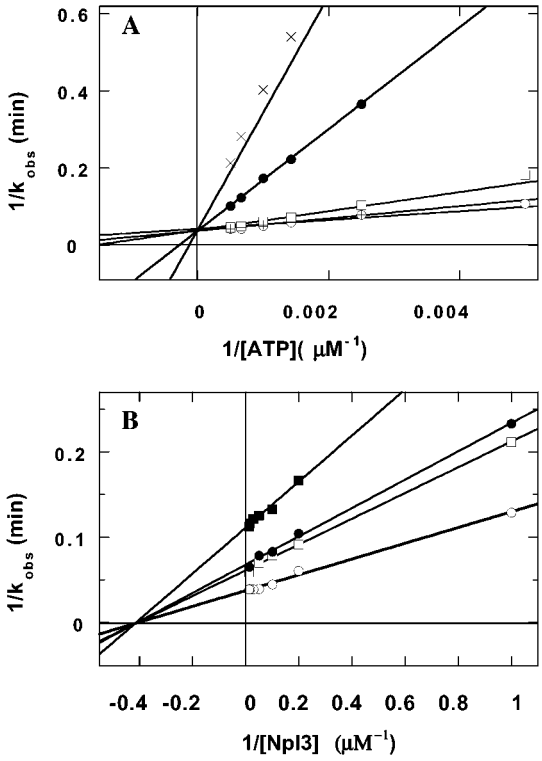

FIGURE 7: Double reciprocal plots of k_{obs} versus ATP or Npl3p concentration in the presence of AMPPNP. (A) Varied [ATP]. The initial rate constants are measured as a function of varied ATP concentrations (10−2000 μM) at varied, fixed concentrations of AMPPNP [1 (×), 0.5 (●), 0.25 (□), 0.10 (+), and 0 mM (○)] and 100 nM Sky1pΔNS. (B) Varied [Npl3p]. The initial rate constants are measured as a function of varied Npl3p concentrations (1−80 μM) at varied, fixed concentrations of AMPPNP [2 (■), 1 (●), 0.5 (□), and 0 mM (○)] and 100 nM Sky1pΔNS.

μM), the rates of the exponential phases are equivalent (k_b = 40 ± 20 s^{-1}). This rate constant is approximately 80-fold higher than k_{cat} (Table 1), indicating that the rate of the phosphoryl transfer step is fast. The amplitudes of the experimental phases increase linearly as a function of Npl3p concentration (Figure 8B). The slightly substoichiometric amount of Npl3p phosphorylation (slope = 0.8) may reflect error in measuring phosphoryl content and/or incomplete saturation of the enzyme with ATP. Using 500 μM ATP, we anticipate that approximately 75% of the available active sites will be occupied, a value close to the measured amplitude (0.8). To determine the true active-site concentration, rapid quench flow studies were performed using excess Npl3p (12 μM) and limiting Sky1pΔNS (1 μM). The kinetic transient obtained under these conditions (Figure 9) is comprised of a rapid exponential phase ('burst' phase) followed by a linear, steady-state phase. The data were fit to eq 3 to obtain values of 0.8 ± 0.1 μM, 30 ± 10 s^{-1}, and 0.7 ± 0.01 μM/s for α, k_b, and L, respectively. Normalizing the linear rate data with the enzyme concentration provides a linear rate constant of 0.7 s^{-1}, a value close to the expected k_{cat} for Npl3p phosphorylation (Table 1).

DISCUSSION

SRPKs are distinguished from other members of the protein kinase family by a large spacer insert within the kinase domain (Figure 1A). In Sky1p, the spacer lies between β strands 7 and 8, a region that is far from the active site

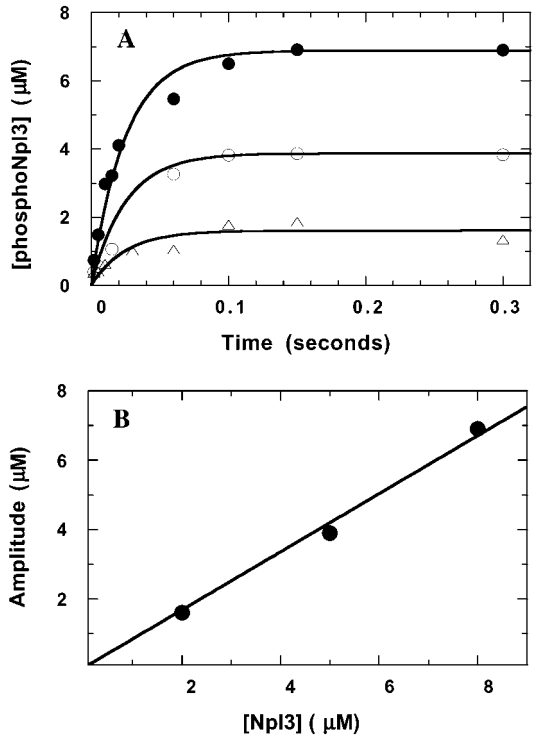

FIGURE 8: Phosphorylation of Npl3p using rapid quench flow methods. (A) Single turnover experiment. Excess Sky1pΔNS (12 μM), preequilibrated with limiting concentrations of Npl3p [2 (△), 5 (○), and 8 μM (●)] and 4 mM free Mg^{2+}, is mixed with ATP (500 μM) in the rapid quench flow instrument. The data are fit to eq 3 where $L = 0$. (B) The amplitude of the exponential phase in panel A is plotted against the total Npl3p concentration. The slope of the line drawn through the data is 0.82.

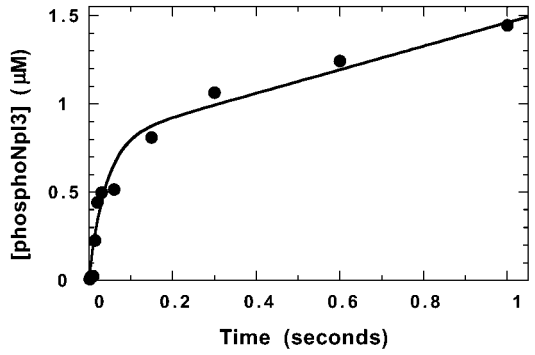

FIGURE 9: Pre-steady-state kinetic transient for the phosphorylation of Npl3p. Sky1pΔNS (1 μM) is preequilibrated with Np13p (12 μM) and 4 mM free Mg^{2+}, and the reaction is initiated with ATP (500 μM). The data are fit to eq 3.

yet is near the linker region between the ATP and substrate binding lobes (*15*). In addition to this large insertion, Sky1p possesses other unique structural features which may account for its constitutive activity (Figure 1B). For instance, the activation loop does not contain a phosphorylation site and, thus, relies on other structural factors for stability. For example, the activation loop appears to be stabilized by close interactions with the C-terminal tail of the protein. Also, a small insertion immediately preceding helix αC (a small helix αC′ not seen in other protein kinases) may stabilize the active form of the enzyme. Both this helix and the activation loop in other protein kinases have been shown to move considerable distances upon catalytic activation (*17*, *18*, *29*). The goals of this kinetic investigation are to establish the fundamental catalytic pathway for Sky1p using both steady-state and pre-steady-state kinetic methods and a natural substrate, Npl3p, and determine whether this unique kinase core imparts unique kinetic properties.

Role of Metal Ions and Ionic Strength in Catalysis. An initial goal in characterizing Sky1p is to understand the role of metal ions in facilitating substrate phosphorylation. Protein kinases typically use two metal ions for binding ATP and supporting phosphoryl transfer (*27*, *30*−*33*). The primary metal ion binds with high affinity and is essential for catalysis, interacting with either one or two of the ATP phosphates and a conserved aspartic acid (*34*). While protein kinases have been shown to accept different divalent metal ions in this position, Mg^{2+} is considered the physiological metal owing to its high concentration in the cell (*35*). The second metal ion binds with weaker affinity in most cases and may lead to either an increase or a decrease in catalytic activity (*23*). We showed that Sky1pΔNS, like other eukaryotic protein kinases, binds two Mg^{2+} (Figure 2). By comparing the initial velocities of the reaction at stoichiometric metal−ATP concentrations and conditions where metal greatly exceeds the ATP concentration, we conclude that the second metal enhances catalysis by approximately 4-fold (Figure 2).

Some protein kinases respond uniquely to the ionic strength of the assay medium. For example, while the catalytic activity of PKA is not greatly affected by added salts (*36*, *37*), Csk is substantially inactivated by modest amounts of NaCl (*38*). Likewise, approximately 60% of the catalytic activity of Sky1pΔNS is lost at a physiological KCl concentration of 100 mM (Figure 3). Analysis of the steady-state kinetic parameters indicates that this inactivation is due to reduced k_{cat} values with little or no change in the K_m's for substrate and ATP. It is difficult to know why Sky1p and other protein kinases display low activities at physiological salt levels. In general, SRPKs function as components of large protein complexes. In these complexes, large surface areas on Sky1p may be occupied by other protein accessories which shield the enzyme from physiological buffers. Alternatively, the catalytic power of Sky1p may be sufficiently high at 100 mM KCl to accomplish its physiological role. These issues will be better addressed when more information is known about other proteins associated with Sky1p. However, it is clear from our kinetic studies that the association of the natural substrate with Sky1p does not influence this salt effect (Figure 3). Whether the spacer insert influences the electrostatic properties of Sky1p awaits the expression and characterization of the full-length enzyme.

Recognition Elements for Substrate Binding. Sky1p phosphorylates the RNA carrier protein Npl3p in vivo at a single serine (*13*). This phosphorylation promotes dissociation of mRNA from Npl3, leading to transport of Npl3 to the nucleus. To understand how Sky1p recognizes Npl3p, we studied the phosphorylation of Npl3p and a substrate peptide based on the single phosphorylation site in this protein. As shown in Table 1, Npl3p binds approximately 100-fold better than the substrate peptide. However, differences in K_m values may not necessarily reflect comparable differences in real binding affinity. K_m measurements frequently contain information on the nature of the kinetic mechanism. For Sky1pΔNS, if the rate of phosphoryl transfer is fast relative to other steps, the K_m may be considerably lower than K_d

(*19*, *36*). Given this uncertainty, the differences in K_m's for Npl3p and substrate peptide may reflect real differences in binding affinity or an enhanced rate of phosphoryl transfer to the protein substrate compared to the peptide. Thus, Npl3p possesses a higher apparent affinity than the peptide either because it utilizes more binding contacts on Sky1p, resulting in improved affinity, and/or because it better positions the hydroxyl acceptor for efficient delivery of the γ-phosphate of ATP. In either event, the additional determinants on the protein substrate greatly impact recognition.

Cooperativity and Order of Addition. In general, steady-state kinetic studies have demonstrated that protein kinases bind ATP and their respective substrates randomly [see review (*23*)]. Nonetheless, there have been several cases where ATP or substrate has been shown to bind first, enforcing an ordered pathway (*39*−*41*). Most of these order of addition experiments have been performed using short substrate peptides rather than full-length proteins. It is conceivable that the larger protein substrates may influence active-site accessibility in a unique manner compared to the peptides. To investigate this possibility and determine whether Sky1p adopts a random or ordered kinetic mechanism, we utilized a nonhydrolyzable ATP analogue, AMPPNP. As expected, AMPPNP competes for the nucleotide site but displays noncompetitive inhibition with respect to Npl3p (Figure 7). This pattern can be attained only if ATP and Npl3p bind randomly in the active site. Furthermore, while the binding of ATP is impeded by the presence of the substrate peptide, there is no apparent binding synergism between ATP and Npl3p (Figure 5). The X-ray structures for protein kinases reveal a deep catalytic cleft for the nucleotide. How ATP gains entrance to this deep pocket in the presence of a large protein substrate is presently unclear. Movements in the two lobes of the kinase domain may alter the accessibility of the active site (*42*, *43*), allowing ATP to bind despite a bulky substrate nearby. Whatever the molecular underpinnings of this process, it is insightful to know that protein kinases such as Sky1p can recognize large proteins such as Npl3p without obstructing nucleotide binding.

Npl3p Turnover Is Limited by Product Release. Despite the importance of protein kinases for cellular function, few have been studied using detailed fast-mixing kinetic methods. In cases where pre-steady-state kinetic data are available, short peptides rather than physiological protein substrates have been used to monitor phosphorylation and assess catalytic mechanism (*19*−*21*, *44*, *45*). The data derived from these previous studies indicate that the rate of phosphoryl transfer from ATP to the substrate peptide is fast, implying that the release of products and associated conformational changes limit turnover. Whether this mechanism applies to the phosphorylation of physiological substrates has not been tested. These shortcomings stem largely from the difficulty of working with protein substrates. In many cases, the real physiological target or targets for a particular protein kinase are unknown or are not readily obtained in sufficient quantity for detailed mechanistic investigations. We have overcome this problem by expressing and purifying large amounts of the natural substrate, Npl3p, for Sky1p. This recombinant protein is phosphorylated at a single site so that the anticipated kinetic transients should be easily interpreted (Figure 4).

Scheme 1

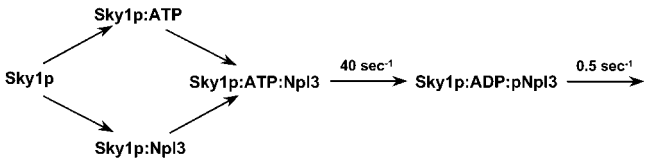

Monitoring the phosphorylation of Npl3p under single turnover conditions allows the direct measurement of the phosphoryl transfer step in the absence of steady-state turnover (*46*). When the enzyme exceeds the substrate concentration, the observed rate of the exponential transient is directly equivalent to the rate of protein phosphorylation in the active site. Since the rate of the exponential transient for this experiment (40 s^{-1}, Figure 8A) greatly exceeds the turnover number (0.5 s^{-1}, Table 1), we conclude that the phosphorylation of Npl3p is not limited by the delivery of the γ-phosphate of ATP. Rather, turnover must be limited by a step or steps after delivery and may include the release of one or both of the products. To provide further support for this mechanism, we performed pre-steady-state kinetic experiments under conditions of excess substrate. Here, we obtained a rapid 'burst' phase that is similar in rate to the single turnover experiment (Figure 9). The linear phase rate of this transient corresponds appropriately with the expected steady-state kinetic parameters in Table 1. Thus, both the single turnover and multiturnover experiments indicate that while Sky1p rapidly phosphorylates Npl3p in the active site (40 s^{-1}), subsequent catalytic cycles are limited by slow product release (0.5 s^{-1}).

CONCLUSION

Through the application of steady-state and pre-steady-state kinetic methods, we have established a catalytic pathway for Sky1p, a yeast homologue of the human SRPKs. The majority of the available steady-state kinetic investigations on protein kinases aimed at determining catalytic mechanism have been performed using short peptide substrates. It is conceivable that larger proteins may enforce ordered processes where the smaller peptides may not be based on steric considerations. As shown in Scheme 1, we demonstrated that Sky1p binds randomly ATP and its natural substrate, Npl3p. Thus, despite its size, Npl3p does not occlude the active site and prevent ATP binding. While it is unclear how this feat is accomplished, Sky1p utilizes an extended active-site surface recognizing residues distal from the immediate phosphorylation site locus. This extended surface not only affords high-affinity protein binding but also diminishes unfavorable contacts in the ternary complex with ATP. Finally, Sky1p rapidly phosphorylates Npl3p, once bound, and then slowly releases products in the rate-determining step for catalysis (Scheme 1). Similar kinetic pathways have also been observed for several other protein kinases (PKA, Csk, and Her-2) (*19*−*21*, *44*, *47*). While PKA and Csk phosphorylate optimal peptide substrates at fast rates (100−500 s^{-1}), Her-2 is less efficient with its substrate (4 s^{-1}). Nonetheless, phosphoryl transfer in the active site does not limit the turnover numbers for these three enzymes with their peptide substrates. Here, we show for the first time that a similar kinetic pathway occurs for a natural protein substrate.

REFERENCES

1. Tarn, W. Y., and Steitz, J. A. (1997) *Trends Biochem. Sci. 22*, 132−137.
2. Hamm, J., and Lamond, A. I. (1998) *Curr. Biol. 8*, R532−R534.
3. Staley, J. P., and Guthrie, C. (1998) *Cell 92*, 315−326.
4. Stojdl, D. F., and Bell, J. C. (1999) *Biochem. Cell Biol. 77*, 293−298.
5. Colwill, K., Pawson, T., Andrews, B., Prasad, J., Manley, J. L., Bell, J. C., and Duncan, P. I. (1996) *EMBO J. 15*, 265−275.
6. Duncan, P. I., Stojdl, D. F., Marius, R. M., Scheit, K. H., and Bell, J. C. (1998) *Exp. Cell Res. 241*, 300−308.
7. Gui, J. F., Tronchere, H., Chandler, S. D., and Fu, X. D. (1994) *Proc. Natl. Acad. Sci. U.S.A. 91*, 10824−10828.
8. Wang, H. Y., Lin, W., Dyck, J. A., Yeakley, J. M., Songyang, Z., Cantley, L. C., and Fu, X. D. (1998) *J. Cell Biol. 140*, 737−750.
9. Cao, W., Jamison, S. F., and Garcia-Blanco, M. A. (1997) *RNA 3*, 1456−1467.
10. Mermoud, J. E., Cohen, P. T., and Lamond, A. I. (1994) *EMBO J. 13*, 5679−5688.
11. Yeakley, J. M., Tronchere, H., Olesen, J., Dyck, J. A., Wang, H. Y., and Fu, X. D. (1999) *J. Cell Biol. 145*, 447−455.
12. Yun, C. Y., and Fu, X. D. (2000) *J. Cell Biol. 150*, 707−718.
13. Gilbert, W., Siebel, C. W., and Guthrie, C. (2001) *RNA 7*, 302−313.
14. Siebel, C. W., Feng, L., Guthrie, C., and Fu, X. D. (1999) *Proc. Natl. Acad. Sci. U.S.A. 96*, 5440−5445.
15. Nolen, B., Yun, C. Y., Wong, C. F., McCammon, J. A., Fu, X. D., and Ghosh, G. (2001) *Nat. Struct. Biol. 8*, 176−183.
16. Andersen, M. D., Shaffer, J., Jennings, P. A., and Adams, J. A. (2001) *J. Biol. Chem. 276*, 14204−14211.
17. Hubbard, S. R. (1997) *EMBO J. 16*, 5572−5581.
18. Jeffrey, P. D., Russo, A. A., Polyak, K., Gibbs, E., Hurwitz, J., Massague, J., and Pavletich, N. P. (1995) *Nature 376*, 313−320.
19. Grant, B. D., and Adams, J. A. (1996) *Biochemistry 35*, 2022−2029.
20. Shaffer, J., Sun, G., and Adams, J. A. (2001) *Biochemistry 40*, 11149−11155.
21. Jan, A. Y., Johnson, E. F., Diamonti, A. J., Carraway, I. K., and Anderson, K. S. (2000) *Biochemistry 39*, 9786−9803.
22. Gill, S. C., and von Hippel, P. H. (1989) *Anal. Biochem 182*, 319−326.
23. Adams, J. A. (2001) *Chem. Rev. 101*, 2271−2290.
24. Grace, M. R., Walsh, C. T., and Cole, P. A. (1997) *Biochemistry 36*, 1874−1881.
25. Cook, P. F., Neville, M. E., Jr., Vrana, K. E., Hartl, F. T., and Roskoski, R., Jr. (1982) *Biochemistry 21*, 5794−5799.
26. Whitehouse, S., Feramisco, J. R., Casnellie, J. E., Krebs, E. G., and Walsh, D. A. (1983) *J. Biol. Chem. 258*, 3693−3701.
27. Adams, J. A., and Taylor, S. S. (1993) *Protein Sci. 2*, 2177−2186.
28. Sun, G., and Budde, R. J. (1997) *Biochemistry 36*, 2139−2146.
29. Russo, A. A., Jeffrey, P. D., and Pavletich, N. P. (1996) *Nat. Struct. Biol. 3*, 696−700.
30. Saylor, P., Wang, C., Hirai, T. J., and Adams, J. A. (1998) *Biochemistry 37*, 12624−12630.
31. Armstrong, R. N., Kondo, H., Granot, J., Kaiser, E. T., and Mildvan, A. S. (1979) *Biochemistry 18*, 1230−1238.
32. Sun, G., and Budde, R. J. (1999) *Biochemistry 38*, 5659−5665.
33. Huang, C. Y., Yuan, C. J., Luo, S., and Graves, D. J. (1994) *Biochemistry 33*, 5877−5883.
34. Zheng, J., Knighton, D. R., Ten Eyck, L. F., Karlsson, R., Xuong, N., Taylor, S. S., and Sowadski, J. M. (1993) *Biochemistry 32*, 2154−2161.
35. Romani, A., and Scarpa, A. (1992) *Arch. Biochem. Biophys. 298*, 1−12.
36. Adams, J. A., and Taylor, S. S. (1992) *Biochemistry 31*, 8516−8522.
37. Adams, J. A., and Taylor, S. S. (1993) *J. Biol. Chem. 268*, 7747−7752.
38. Cole, P. A., Burn, P., Takacs, B., and Walsh, C. T. (1994) *J. Biol. Chem. 269*, 30880−30887.
39. LoGrasso, P. V., Frantz, B., Rolando, A. M., O'Keefe, S. J., Hermes, J. D., and O'Neill, E. A. (1997) *Biochemistry 36*, 10422−10427.
40. Parast, C. V., Mroczkowski, B., Pinko, C., Misialek, S., Khambatta, G., and Appelt, K. (1998) *Biochemistry 37*, 16788−16801.
41. Erneux, C., Cohen, S., and Garbers, D. L. (1983) *J. Biol. Chem. 258*, 4137−4142.
42. Cox, S., Radzio-Andzelm, E., and Taylor, S. S. (1994) *Curr. Opin. Struct. Biol. 4*, 893−901.
43. Williams, J. C., Weijland, A., Gonfloni, S., Thompson, A., Courtneidge, S. A., Superti-Furga, G., and Wierenga, R. K. (1997) *J. Mol. Biol. 274*, 757−775.
44. Shaffer, J., and Adams, J. A. (1999) *Biochemistry 38*, 12072−12079.
45. Shaffer, J., and Adams, J. A. (1999) *Biochemistry 38*, 5572−5581.
46. Johnson, K. A. (1998) *Curr. Opin. Biotechnol. 9*, 87−89.
47. Zhou, J., and Adams, J. A. (1997) *Biochemistry 36*, 2977−2984.

BI020233Y